J. Fluid Mech. (1997), *vol.* 333, *pp.* 231–255

Copyright © 1997 Cambridge University Press

An ideal fluid jet impinging on an uneven wall

By WEIDONG PENG† AND DAVID F. PARKER

Department of Mathematics and Statistics, University of Edinburgh,
The King's Buildings, Edinburgh EH9 3JZ, UK

(Received 27 July 1993 and in revised form 13 August 1996)

The two-dimensional free-surface problem of an ideal jet impinging on an uneven wall is studied using complex-variable and transform techniques. A relation between the flow angle on the free surface and the wall angle is first obtained. Then, by using a Hilbert transform and the generalized Schwarz–Christoffel transformation technique, a system of nonlinear integro-differential equations for the flow angle and the wall angle is formulated. For the case of symmetric flow, a compatibility condition for the system is automatically satisfied. In some special cases, for instance when the wall is a wedge, the problem reduces to the evaluation of several integrals. Moreover, in the case of a jet impinging normally on a flat wall, the classical result is recovered. For the asymmetric case, a relation is obtained between the point in the reference ζ-plane which corresponds to the position of the stagnation point in the physical plane, the flow speed and the shape of the wall. The solution to a linearized problem is given, for comparison. Some numerical solutions are presented, showing the shape of the free surface corresponding to a number of different wall shapes.

1. Introduction

The problem of determining the free surface of a two-dimensional jet of ideal fluid impinging on an uneven wall is considered. The application of such a fluid jet can be found in the formation of glassy metals (Jenkins & Barton 1989) and heat transfer from a fluid to a curved solid surface (see Martin 1977; Stevens & Webb 1992). The classical problem of free streamline flow of an ideal fluid has been studied by many authors. Early work in this area is characterized by the use of the hodograph method and the Schwarz–Christoffel formula, which can deal with flows which have a polygonal boundary geometry or whose hodograph plane is a polygon of simple shape. Surveys of the hodograph method applied to jet theory can be found in Birkhoff & Zarantonello (1957), Gurevich (1965) and Woods (1961). The requirement of the polygonal geometric shape limits the application of the method in practical problems. Woods (1958, 1961) gave some generalizations of the Schwarz–Christoffel formula which can be used to transform a half-plane into a domain with a boundary which combines a polygon and a smooth curve. By using the generalized formula, Dobroval'skaya (1969) derived a nonlinear singular integral equation for the water wedge entry problem, Bloor (1978) obtained an integro-differential equation for studying the problem of large-amplitude periodic water waves and, more recently,

† Present address: Department of Mathematics and Statistics, University of Paisley, High Street, Paisley, PA1 2BE, UK.

https://doi.org/10.1017/S0022112096004399 Published online by Cambridge University Press

King & Bloor considered various flow problems such as free-surface flows over a step (1987), free-surface flows over an arbitrary bed topography, and the cusped free-surface flows due to a submerged source (1990). A general feature of the work in the cited papers is that the complex potential must be determined in the reference ζ-plane corresponding to the fluid domain. Some numerical solutions describing an ideal jet issuing from polygonal containers and free-streamline problems using complex-variable methods can be found in the work of Dias, Elcrat & Trefethen (1987) describing flow over a weir and in a waterfall by Dias & Tuck (1991), and describing a jet flowing from a slit in a vertical wall by Tuck (1987). Ideal jet flow with gravity was studied by Dias & Christodoulides (1991) and fluid, under gravity, emerging from a two-dimensional nozzle at an angle was considered in the work of Dias & Vanden-Broeck (1990).

In the case of a jet of ideal fluid with other boundary conditions, Jenkins & Barton (1989), based on the Baiocchi transformation, gave a numerical treatment of the impact of a jet on a porous wall. King (1990) extended the classical hodograph method and reduced the same problem to a first-order differential equation.

A two-dimensional ideal jet impinging on an uneven wall, neglecting gravitational body forces is investigated in this study. Motivation comes from the need to study an ideal jet impinging on hemispherical cups and to better understand a jet impinging on an uneven wall. After use of the Hilbert transform, the condition of constant speed on the free streamlines results in a relation between the flow angle on the free surface and the wall angle, when expressed in terms of the coordinate along the real axis of an appropriate reference plane. Then, by combining this with application of the generalized Schwarz–Christoffel transformation technique, a system of nonlinear integro-differential equations for the flow angles and the wall angles is formulated. For the case in which the wall geometry and flow are symmetric, a compatibility condition for the system is automatically satisfied. More generally, for an ideal jet impinging asymmetrically on an uneven wall, the unknown position of the stagnation point introduces much difficulty to the computation of the free-surface shapes. Using the integral form of the momentum equation, we obtain an integral relation between the image in the ζ-plane of the stagnation point in the physical plane, the flow speed and the shape of the wall. The linearized problem is investigated and its analytic solution is given. Some numerical solutions to the resulting nonlinear system are presented, showing the shapes of the free surface corresponding to a number of different wall shapes.

2. Mathematical formulation

The two-dimensional steady irrotational flow of an incompressible inviscid fluid impinging upon an uneven wall is considered (see figure 1). Cartesian coordinates are introduced with the X-axis along the centreline of the approaching jet. The complex variable $Z = X + \mathrm{i}Y$ is introduced.

Far away from the wall, the incident flow is required to be a uniform stream with constant speed U and thickness $2H$. Far away from the stagnation point upward and downward along the wall, the flow is also a uniform stream and thicknesses there are H_1 and H_2 respectively. By the conservation of mass, we have $H_1 + H_2 = 2H$. A velocity potential denoted by Φ and a stream function denoted by Ψ are defined such that the complex potential

$$W = \Phi + \mathrm{i}\Psi$$

https://doi.org/10.1017/S0022112096004399 Published online by Cambridge University Press

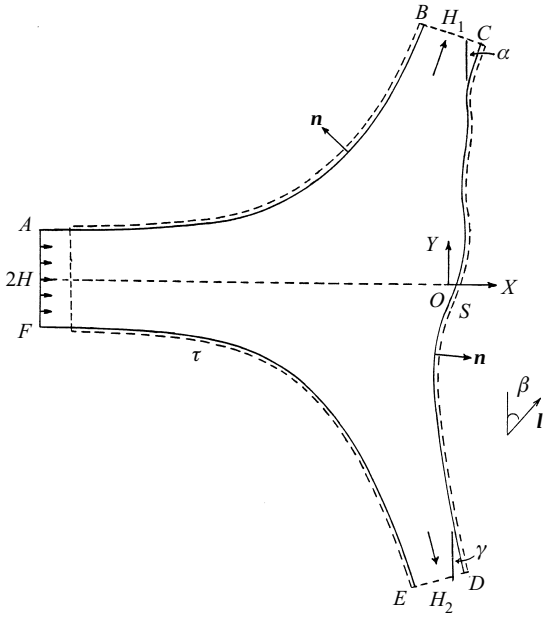


FIGURE 1. A sketch of a jet impinging asymmetrically on a wall.

is analytic in the domain occupied by the fluid. Bernoulli's equation is applied to both free surfaces on which pressure is constant, so that the fluid speed q takes the constant value U there. Meanwhile the stream function Ψ is chosen to have the value UH on the upper free surface, $-UH$ on the lower free surface, and takes the value $\Psi = \Psi_0 = U(H - H_1)$ on the dividing streamline and the wall. For symmetric flows $\Psi_0 = 0$. The complex velocity is defined as

$$V = Uq\mathrm{e}^{-\mathrm{i}\theta}$$

where θ is the angle between the flow direction and the X-axis. The relation between the complex potential and the complex velocity is given by

$$\frac{\mathrm{d}W}{\mathrm{d}Z} = V.$$

This problem is now non-dimensionalized using the substitutions

$$z = x + \mathrm{i}y = \frac{X + \mathrm{i}Y}{H}, \quad w = \phi + \mathrm{i}\psi = \frac{\Phi + \mathrm{i}\Psi}{UH}, \quad v = q\mathrm{e}^{-\mathrm{i}\theta} = \frac{V}{U} \tag{2.1}$$

and by then writing $H_1 = Hh_1$, $H_2 = Hh_2$, so that $h_1 + h_2 = 2$, where ψ is respectively ± 1 on the upper and lower free surfaces.

We introduce the function ω as follows:

$$\omega = \log v = \log q - \mathrm{i}\theta. \tag{2.2}$$

3. Flow angles

We seek a mapping of the flow region in the z-plane onto the upper half of a transform plane $\zeta = \xi + \mathrm{i}\eta$ (the reference, or *canonical* domain) and then seek ω as a

https://doi.org/10.1017/S0022112096004399 Published online by Cambridge University Press

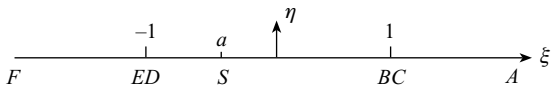


FIGURE 2. The $\zeta = \xi + i\eta$ plane.

function of ζ there (see figure 2). Since ω is an analytic function of ζ, the values of $\log q$ and θ on the axis $\eta = 0$ are related as Hilbert transforms, so giving

$$q(\xi) = \exp\left\{\frac{1}{\pi}\fint_{-\infty}^{\infty}\frac{\theta(t)}{\xi - t}\mathrm{d}t\right\}$$

where $\fint$ denotes a principal value integral. Since $q = 1$ on the free surface, this gives

$$\frac{1}{\pi}\fint_{-\infty}^{\infty}\frac{\theta(t)}{\xi - t}\mathrm{d}t = 0, \qquad 1 <| \xi |< \infty. \tag{3.1}$$

We now define the function $F(\xi)$ by

$$F(\xi) = \frac{1}{\pi}\int_{-1}^{1}\frac{\theta(t)}{\xi - t}\mathrm{d}t, \qquad 1 <| \xi |< \infty, \tag{3.2}$$

so that equation (3.1) becomes

$$\frac{1}{\pi}\fint_{-\infty}^{-1}\frac{\theta(t)}{\xi - t}\mathrm{d}t + \frac{1}{\pi}\fint_{1}^{\infty}\frac{\theta(t)}{\xi - t}\mathrm{d}t = -F(\xi), \qquad 1 <| \xi |< \infty. \tag{3.3}$$

Making the change of variables $t = r^{-1}$, $\quad s = \xi^{-1}$ in (3.3) gives

$$\begin{aligned} -F(s^{-1}) &= \frac{1}{\pi}\fint_{-1}^{0}\frac{s\theta(r^{-1})r^{-1}}{r - s}\mathrm{d}r + \frac{1}{\pi}\fint_{0}^{1}\frac{s\theta(r^{-1})r^{-1}}{r - s}\mathrm{d}r \\ &= \frac{s}{\pi}\fint_{-1}^{1}\frac{\theta(r^{-1})r^{-1}}{r - s}\mathrm{d}r, \qquad 0 < |s| < 1. \end{aligned} \tag{3.4}$$

Similarly, substituting for ξ in (3.2) gives

$$F(\xi) = F(s^{-1}) = s\frac{1}{\pi}\int_{-1}^{1}\frac{\theta(t)}{1 - st}\mathrm{d}t = sg(s), \qquad 0 < |s| < 1, \tag{3.5}$$

where $g(s)$ is defined by

$$g(s) = \frac{1}{\pi}\int_{-1}^{1}\frac{\theta(t)}{1 - st}\mathrm{d}t, \qquad 0 < |s| < 1. \tag{3.6}$$

Combining (3.4) and (3.5) then yields the so-called aerofoil equation

$$g(s) = \frac{1}{\pi}\fint_{-1}^{1}\frac{\phi(r)}{s - r}\mathrm{d}r, \qquad 0 < |s| < 1, \tag{3.7}$$

which here relates $g(s)$ defined by (3.6) in terms of the flow angle on the wall to $\phi(r) \equiv r^{-1}\theta(r^{-1})$. In order to invert the integral equation (3.7), we first show in Appendix A that $g(s)$ defined by (3.6) is square integrable. Then (see Hochstadt 1973) one obtains

$$\phi(s) = \frac{c}{(1 - s^2)^{1/2}} - \frac{1}{\pi}\fint_{-1}^{1}\left(\frac{1 - r^2}{1 - s^2}\right)^{1/2}\frac{g(r)}{s - r}\mathrm{d}r, \tag{3.8}$$

https://doi.org/10.1017/S0022112096004399 Published online by Cambridge University Press

where c is a constant to be determined later. Moreover, there is an alternative representation

$$\phi(s) = -\frac{1}{\pi}\fint_{-1}^{1}\left(\frac{1-s^2}{1-r^2}\right)^{1/2}\frac{g(r)}{s-r}\mathrm{d}r \tag{3.9}$$

valid subject to the compatibility condition

$$\int_{-1}^{1}\frac{g(s)}{(1-s^2)^{1/2}}\mathrm{d}s = 0. \tag{3.10}$$

Reinterpreting (3.8) in terms of the free-streamline angle $\theta(s^{-1}) = s\phi(s)$ gives

$$s^{-1}\theta(s^{-1})(1-s^2)^{1/2} = c - \fint_{-1}^{1}(1-r^2)^{1/2}\frac{g(r)}{s-r}\mathrm{d}r. \tag{3.11}$$

Since θ remains finite as $s \to \pm 1$, we obtain the two expressions

$$c = \int_{-1}^{1}(1-r^2)^{1/2}\frac{g(r)}{1-r}\mathrm{d}r = -\int_{-1}^{1}(1-r^2)^{1/2}\frac{g(r)}{1+r}\mathrm{d}r,$$

from which we find that

$$0 = \int_{-1}^{1}\left(1-r^2\right)^{1/2}\left(\frac{1}{1-r}+\frac{1}{1+r}\right)g(r)\mathrm{d}r = 2\int_{-1}^{1}\frac{g(r)}{(1-r^2)^{1/2}}\mathrm{d}r.$$

Consequently condition (3.10) is satisfied for all wall shapes. Equation (3.11) may be rewritten in terms of $\theta(t)$ ($|t| > 1$) as (see Appendix B)

$$\theta(t) = \pm\frac{1}{\pi}\frac{\left(t^2-1\right)^{1/2}}{t}\left(\fint_{-\infty}^{-1} - \fint_{1}^{\infty}\right)\frac{1}{\left(\xi^2-1\right)^{1/2}}\frac{\xi F(\xi)}{\xi - t}\mathrm{d}\xi, \qquad |t| > 1, \tag{3.12}$$

where the positive sign applies for $t > 1$ and the negative sign for $t < -1$. Equation (3.12), combined with (3.2), gives a linear relation between the flow angle on the free surface and on the wall in a closed form, but specified in terms of the parameter ξ on the real axis of the ζ-plane.

4. The governing equations

The geometry of the flow region together with the free surface and typical curved wall boundary is shown in figure 1. The transformation of this region to the canonical domain is given by the generalized Schwarz–Christoffel formula

$$\frac{\mathrm{d}z}{\mathrm{d}\zeta} = -\frac{2}{\pi}\frac{\zeta - a}{\zeta^2 - 1}\exp\left(-\frac{1}{\pi}\int_{-\infty}^{\infty}\frac{\theta(t)}{\zeta - t}\mathrm{d}t\right), \qquad \zeta = \xi + \mathrm{i}\eta, \quad \eta \geqslant 0, \tag{4.1}$$

where $\theta(t)$ is the flow angle on either the free surface or the wall, and where the real value a defines the image in the ζ-plane of the stagnation point of the flow. This is obtained from a generalization (see Woods 1958, 1961) of the Schwarz–Christoffel mapping formula with adjustment to allow for the sense of the tangent direction along the boundary. Letting $\eta \to 0^+$ modifies equation (4.1) as

$$\frac{\mathrm{d}z}{\mathrm{d}\xi} = -\frac{2}{\pi}\frac{\xi - a}{\xi^2 - 1}\exp\left(-\frac{1}{\pi}\fint_{-\infty}^{\infty}\frac{\theta(t)}{\xi - t}\mathrm{d}t + \mathrm{i}\theta(\xi)\right). \tag{4.2}$$

https://doi.org/10.1017/S0022112096004399 Published online by Cambridge University Press

Integrating this equation and then taking the imaginary part gives

$$y(t) = y(a) + \frac{2}{\pi}\int_a^t \frac{\xi - a}{1-\xi^2} \exp\left(-\frac{1}{\pi}\fint_{-\infty}^{\infty} \frac{\theta(u)}{\xi - u}\mathrm{d}u\right) \sin\theta(\xi)\mathrm{d}\xi, \qquad |\,t\,| < 1,$$

on the wall. If the equation for the wall is $x = k(y)$, then the inclination of the wall to the x-axis is $\theta_w = \pi/2 - \tan^{-1}\kappa'(y)$, which may be used with (4.2) to relate θ to the parameter t through

$$\theta(t) = \pm\frac{\pi}{2} - \tan^{-1}\kappa'\left(y(a) + \frac{2}{\pi}\int_a^t \frac{\xi - a}{1-\xi^2} \exp\left(-\frac{1}{\pi}\fint_{-\infty}^{\infty} \frac{\theta(u)}{\xi - u}\mathrm{d}u\right) \sin\theta(\xi)\mathrm{d}\xi\right). \tag{4.3}$$

Here the upper and lower signs apply for $a < t < 1$ and for $-1 < t < a$, respectively, since the flow angle $\theta(t)$ is related to the wall angle $\theta_w(t)$ by

$$\theta(t) = \begin{cases} \theta_w(t), & a < t < 1, \\ \theta_w(t) - \pi, & -1 < t < a. \end{cases} \tag{4.4}$$

Equations (3.2), (3.12) and (4.3) form a system of nonlinear integro-differential equations for this problem. If this system is solved for $\theta(t)$, $|t| < 1$, then $F(\xi)$, $|\xi| > 1$, is given by (3.2) and $\theta(t)$ for $|t| > 1$ is obtained from equation (3.12). The mapping from the ζ-plane to the physical plane is given by (4.1). The shape of the free surface is determined by (4.2), which, in view of condition (3.1), reduces to

$$\frac{\mathrm{d}z}{\mathrm{d}\xi} = -\frac{2}{\pi}\frac{\xi - a}{\xi^2 - 1}\exp\left(\mathrm{i}\theta(\xi)\right), \qquad 1 < |\xi| < \infty. \tag{4.5}$$

It is unlikely that this system of equations can be solved analytically except for special cases of $\kappa(y)$. In the following section we discuss some of these.

5. Some special cases

If the t-dependence of the flow angle on the wall is known, $F(\xi)$ is given explicitly by equation (3.2), so that the free-streamline shape is computed from (4.5) using expression (3.12) for the flow angle. In these cases, there is no need to solve the system of integral equations. Examples are:

(i) *A jet impinging on an inclined wall at angle* α. Labelling the stagnation point as $\zeta = a$ (to be related to α in §9) reduces equation (3.2) to

$$F(\xi) = \frac{\alpha}{\pi}\log\frac{\xi - a}{\xi - 1} + \left(\frac{\alpha}{\pi} - 1\right)\log\frac{\xi + 1}{\xi - a}, \qquad 1 <|\,\xi\,| < \infty. \tag{5.1}$$

(ii) *A jet impinging symmetrically on an infinite wedge of angle* 2α. This is a special case of the situation $\theta(t) = -\theta(-t)$, $0 < t < 1$ for which $k(y)$ is odd and $F(\xi)$ is even, so reducing equation (3.2) to

$$F(\xi) = \frac{2}{\pi}\int_0^1 \frac{t\theta(t)}{\xi^2 - t^2}\mathrm{d}t, \qquad 1 <|\,\xi\,| < \infty. \tag{5.2}$$

Setting $\theta(t) = \alpha$ in equation (5.2) then gives

$$F(\xi) = \frac{\alpha}{\pi}\log\frac{\xi^2}{\xi^2 - 1}.$$

(iii) *A jet impinging normally on an infinite wall.* This special case of both (i) and

https://doi.org/10.1017/S0022112096004399 Published online by Cambridge University Press

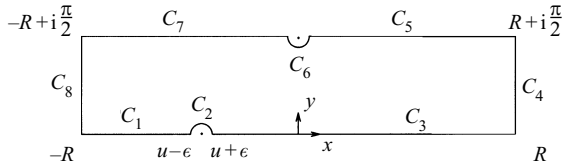


FIGURE 3. The path of integration C.

(ii) ($\theta(t) = \alpha = \pi/2$, $0 < t < 1$) gives

$$F(\xi) = \frac{1}{2}\log\frac{\xi^2}{\xi^2 - 1}. \tag{5.3}$$

More generally, for symmetric flows leading to (5.2) it is natural to choose $y(a) = 0$, while $\theta(t) = \theta_w(t)$ on $0 < t < 1$. Then, equation (4.3) becomes

$$\theta(t) = \frac{\pi}{2} - \tan^{-1}\kappa'\left(\frac{2}{\pi}\int_0^t \frac{\xi}{1-\xi^2}\,P(\xi)\sin\theta(\xi)\mathrm{d}\xi\right), \qquad 0 < t < 1, \tag{5.4}$$

where $P(\xi)$ is defined as

$$P(\xi) = \exp\left(-\frac{2}{\pi}\int_0^\infty \frac{u\theta(u)}{\xi^2 - u^2}\mathrm{d}u\right), \qquad 0 < \xi < t. \tag{5.5}$$

Taking the real and imaginary parts of equation (4.5) gives the shape of the streamline forming the upper portion of the free surface as

$$\frac{\mathrm{d}x}{\mathrm{d}\xi} = -\frac{2}{\pi}\frac{\xi}{\xi^2-1}\cos\theta(\xi), \qquad \frac{\mathrm{d}y}{\mathrm{d}\xi} = -\frac{2}{\pi}\frac{\xi}{\xi^2-1}\sin\theta(\xi), \qquad \xi > 1. \tag{5.6}$$

For numerical computation, it is preferable to exploit the evenness in (3.12) and to apply the substitutions $t^2 - 1 = \mathrm{e}^{2u}$, $\xi^2 - 1 = \mathrm{e}^{2v}$ where $-\infty < u, v < \infty$ for $1 < t, \xi < \infty$. This then yields

$$\theta\left[\left(1+\mathrm{e}^{2u}\right)^{1/2}\right] = \frac{1}{\pi}\int_{-\infty}^{\infty} \frac{F\left[\left(1+\mathrm{e}^{2v}\right)^{1/2}\right]\mathrm{d}v}{\sinh(u-v)}, \qquad -\infty < u < \infty, \tag{5.7}$$

while equations (5.6) give an alternative parametrization

$$x(u) = x(u_0) - \frac{2}{\pi}\int_{u_0}^{u} \cos\theta\left(\left(1+\mathrm{e}^{2u}\right)^{1/2}\right)\mathrm{d}u, \tag{5.8}$$

$$y(u) = y(u_0) - \frac{2}{\pi}\int_{u_0}^{u} \sin\theta\left(\left(1+\mathrm{e}^{2u}\right)^{1/2}\right)\mathrm{d}u \tag{5.9}$$

of the free surface of the jet.

This representation also proves useful for determining analytically the free surface in case (iii). Substituting $\zeta^2 = 1 + \mathrm{e}^{2v}$ into (5.3) gives $F\left[\left(1+\mathrm{e}^{2v}\right)^{1/2}\right] = \frac{1}{2}\log(1+\mathrm{e}^{2v})$ in (5.7). The improper integral is evaluated by considering the indented rectangular contour C of figure 3, with the multivalued function $\frac{1}{2}\log(1+\mathrm{e}^{-2v})$ chosen on the

https://doi.org/10.1017/S0022112096004399 Published online by Cambridge University Press

branch for which, on Im $(v) = 0$, $\arg\log(1 + e^{-2z}) = 0$ and on Im $(v) = i\frac{1}{2}\pi$,

$$\log(1 + e^{-2(x+i\pi/2)}) = \begin{cases} \log(1 - e^{-2x}), & x > 0 \\ \log(e^{-2x} - 1) - i\pi, & x < 0. \end{cases}$$

Then (see Appendix C) it is found that

$$\theta\left(\left(1 + e^{2u}\right)^{1/2}\right) = \frac{1}{2}\int_0^{-\infty} \frac{1}{\cosh(u - x)} dx = \lim_{R\to\infty} \int_{e^{-R-u}}^{e^{-u}} \frac{ds}{1 + s^2}$$
$$= \tan^{-1} e^{-u}$$

or $\tan\theta = (\xi^2 - 1)^{-1/2}$, so that $\sin\theta = \xi^{-1}$, $\cos\theta = (1 - \xi^{-2})^{1/2}$, which satisfy the required asymptotic conditions $\theta \to \pi/2$ as $\xi \to 1$, $\theta \to 0$ as $\xi \to \infty$.

Substituting these into (5.6) gives $dx/d\xi = -2\pi^{-1}(\xi^2 - 1)^{-1/2}$ and $dy/d\xi = -2\pi^{-1}(\xi^2 - 1)^{-1}$. These are best integrated in terms of θ, setting $x = -1$ for $\theta = \pi/2$ and $y = 1$ for $\theta = 0$, as

$$x(\theta) = -1 + \frac{2}{\pi}\int_{\pi/2}^{\theta} \frac{d\tilde{\theta}}{\sin\tilde{\theta}} = -1 + \frac{2}{\pi}\log\tan\frac{\theta}{2}, \tag{5.10}$$

$$y(\theta) = 1 + \frac{2}{\pi}\int_0^{\theta} \frac{d\tilde{\theta}}{\cos\tilde{\theta}} = 1 + \frac{2}{\pi}\log\tan\left(\frac{\pi}{4} + \frac{\theta}{2}\right), \tag{5.11}$$

which are exactly the form of the parametric representation given by Milne-Thomson (1968) for a jet impinging normally on a flat plate, so providing a check on the reformulation presented in §6.

Similarly, for case (ii) of a jet impinging symmetrically on an infinite wedge with angle 2α, we find that $\theta\left((1 + e^{2u})^{1/2}\right) = (2\alpha/\pi)\tan^{-1} e^{-u}$, so that the analytic solutions can also be found by procedures similar to those leading to (5.10) and (5.11).

6. Numerical solutions

In this section numerical solutions are obtained for the symmetric case. The integral in (5.2) is discretized by the trapezoidal rule, using step length δ, with mesh points $t_k = k\delta$, $\theta_k = \theta(k\delta)$, $\xi_j > 1$, $k = 0, 1, ..., N$ with $N\delta = 1$, so giving

$$F_j = F(\xi_j) \simeq \frac{2\delta}{\pi}\sum_{k=0}^{N} w_k \frac{t_k\theta_k}{\xi_j^2 - t_k^2}, \qquad \xi_j > 1, \tag{6.1}$$

with error $O(\delta^2)$, where the w_k are chosen as the weights appropriate to the trapezoidal rule.

The integral in (5.7) is complicated by the singularities at the point $u_j = v_j$ and by the infinite range of integration. The infinite range is accommodated by splitting the range of integration in (5.7) into three parts $(-\infty, -B)$, $(-B, A)$ and (A, ∞), for u in some interval $-l < u < m$, with values of A and B of, for instance, $3m$ and $3l$ respectively. For $\xi^2 = e^{2v} + 1$, $v > M$, the function $F(\xi)$ has the behaviour

$$F(\xi) = \frac{2}{\pi}\int_0^1 \frac{t\theta(t)}{\xi^2 - t^2} dt$$
$$= C\xi^{-2} + O(\xi^{-4}), \quad \text{with} \quad C = \frac{2}{\pi}\int_0^1 t\theta(t) dt.$$

https://doi.org/10.1017/S0022112096004399 Published online by Cambridge University Press

Substituting this into the right-hand side of (5.7) gives the contribution

$$\begin{aligned}\frac{\mathrm{e}^u}{\pi}\int_A^\infty \frac{2}{\mathrm{e}^{2u}-\mathrm{e}^{2v}}F\left[\left(1+\mathrm{e}^{2v}\right)^{1/2}\right]\mathrm{e}^v\mathrm{d}v &\simeq \frac{C\mathrm{e}^u}{\pi}\int_A^\infty \frac{2\mathrm{e}^v\mathrm{d}v}{(\mathrm{e}^{2u}-\mathrm{e}^{2v})(1+\mathrm{e}^{2v})}\\ &= \frac{C\mathrm{e}^u}{\pi}\int_A^\infty \frac{1}{1+\mathrm{e}^{2u}}\left(\frac{1}{1+\mathrm{e}^{2v}}+\frac{1}{\mathrm{e}^{2u}-\mathrm{e}^{2v}}\right)\mathrm{e}^v\mathrm{d}v\\ &\leqslant \frac{C}{\pi}\frac{1+\mathrm{e}^u}{1+\mathrm{e}^{2u}}\mathrm{e}^{u-A}. \end{aligned} \tag{6.2}$$

A similar treatment applied to (5.7) over the interval $(-\infty, -B)$ gives

$$\frac{\mathrm{e}^u}{\pi}\int_{-\infty}^{-B} \frac{2}{\mathrm{e}^{2u}-\mathrm{e}^{2v}}F\left[\left(1+\mathrm{e}^{2v}\right)^{1/2}\right]\mathrm{e}^v\mathrm{d}v \leqslant \frac{C}{\pi}\frac{\mathrm{e}^{u-B}\left(2+\mathrm{e}^{-u}\right)}{1+\mathrm{e}^{2u}}. \tag{6.3}$$

Thus, it is readily shown that the sum of the two contributions to (5.7) given by the left-hand sides of (6.2) and (6.3) has upper bound

$$\frac{C}{\pi}\left(\frac{\mathrm{e}^u+\mathrm{e}^{2u}}{1+\mathrm{e}^{2u}}\mathrm{e}^{-A}+\frac{1+2\mathrm{e}^u}{1+\mathrm{e}^{2u}}\mathrm{e}^{-B}\right) \leqslant \frac{2C}{\pi}\left(\mathrm{e}^{-A}+\mathrm{e}^{-B}\right), \tag{6.4}$$

so giving

$$\theta\left[\left(1+\mathrm{e}^{2u}\right)^{1/2}\right] = \frac{\mathrm{e}^u}{\pi}\int_{-B}^{A}\frac{1}{\mathrm{e}^{2u}-\mathrm{e}^{2v}}F\left[\left(1+\mathrm{e}^{2v}\right)^{1/2}\right]\mathrm{e}^v\mathrm{d}v + O\left(\mathrm{e}^{-A}+\mathrm{e}^{-B}\right). \tag{6.5}$$

The portion $[-B, A]$ of the range of integration is further divided into three subranges $[-B, u_{j-1}]$, $[u_{j-1}, u_{j+1}]$ and $[u_{j+1}, A]$. The integrand in (6.5) is regular and can be dealt with by the trapezoidal rule, except in $[u_{j-1}, u_{j+1}]$ where it is approximated by using the Taylor expansion around the point u_j. This yields

$$\begin{aligned}\Theta(u_j) \equiv \theta\left[(1+\mathrm{e}^{2u_j})^{1/2}\right] \simeq \frac{\mathrm{e}^{u_j}}{\pi}\Bigg(&\sum_{i=j+1}^{A}\frac{W_i\Delta}{\mathrm{e}^{2u_j}-\mathrm{e}^{2v_i}}F\left[(1+\mathrm{e}^{2v_i})^{1/2}\right]\mathrm{e}^{v_i}\\ &+\sum_{i=-B}^{j-1}\frac{W_i\Delta}{\mathrm{e}^{2u_j}-\mathrm{e}^{2v_i}}F\left[(1+\mathrm{e}^{2v_i})^{1/2}\right]\mathrm{e}^{v_i}\\ &+\left(-\frac{\Delta}{2}+\log\frac{1+\mathrm{e}^{\Delta/2}}{1+\mathrm{e}^{-\Delta/2}}\right)F\left[(1+\mathrm{e}^{2u_j})^{1/2}\right]+\Delta\frac{F_j'\mathrm{e}^{2u_j}}{(1+\mathrm{e}^{2u_j})^{1/2}}\Bigg)\end{aligned} \tag{6.6}$$

where Δ is the step length, $u_j = j\Delta$ for $j = -L, ..., M$ with $-L\Delta = -l$, $M\Delta = m$, and W_i are the weights appropriate to the trapezoidal rule used for (6.5). The function F_j' is the derivative of F_j and can be calculated from (5.2).

The integral in equation (5.4) can also be dealt with by the same trapezoidal rule as used in (5.2) so giving

$$\theta_k \simeq \frac{\pi}{2} - \tan^{-1}\kappa'\left(-\frac{2\delta}{\pi}\sum_{n=1}^{k}\frac{\tau_n}{\tau_n^2-1}P_n\sin(\theta_n)\right), \quad k = 0, 1, ..., N \tag{6.7}$$

where $\tau_n = n\delta$, for $n = 0, 1, ..., k$. The quantities P_l are the discretized forms of the function $P(\xi)$, with the singularities at points $\xi = t$, $0 < t < 1$, treated by the same

https://doi.org/10.1017/S0022112096004399 Published online by Cambridge University Press

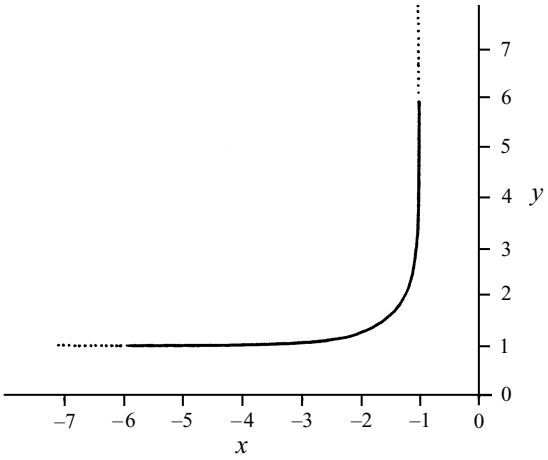


FIGURE 4. One half of a symmetric jet impinging normally on a flat wall $x = 0$; the solid curve represents the analytic result (6.2), (6.3), the dotted curve represents the numerical solution.

method as used in dealing with the integral in (6.5). This gives

$$P_n = P(\tau_n) \simeq \exp\left(-\frac{2}{\pi}\left[\delta \sum_{k=1,k\neq n}^{N} \frac{t_k\theta_k}{\tau_n^2 - t_k^2} - \theta_n' + \Delta \sum_{j=-L}^{M} \frac{(\xi_j^2 - 1)\Theta(u_j)}{\tau_n^2 - \xi_j^2}\right]\right), \quad 0 < \xi < t \tag{6.8}$$

where $\xi_j^2 = 1 + \exp(2u_j)$. Moreover θ' is the first derivative of θ and can be calculated by a central difference approximation with error $O(\delta^2)$ while Θ is given by (6.6). Equations (5.8) and (5.9), discretized by a trapezoidal rule, give

$$x(\xi_i) = x(1) - \frac{\Delta}{\pi} \sum_{j=-L}^{i} \cos\Theta(u_j), \tag{6.9}$$

$$y(\xi_i) = y(\infty) + \frac{\Delta}{\pi} \sum_{j=i}^{M} \sin\Theta(u_j) \tag{6.10}$$

for $i = -L, ..., M$. Thus we obtain $N + 1$ nonlinear algebraic equations for $N + 1$ unknowns from (6.7), combined with equations (6.5), (6.6) and (6.7). This system of equations was solved by using a hybrid Powell method from the NAG library. Equations (6.9) and (6.10) were then used to locate the free streamline.

In figure 4, we give a comparison with the analytic solution for the case of a jet impinging normally on a flat wall. The free-surface shape plotted as a dotted line obtained by using (5.4), (5.7), (5.8) and (5.9) shows good agreement with the analytic result (Milne-Thomson 1968) shown here by the solid line. In the case of an uneven wall, we chose functions $x = e^{-y^2}$, $x = -e^{-y^2}$ and $x = -\text{sech } y$ to describe the wall shape. The step lengths chosen were $\delta = 0.05$, $\Delta = 0.04$ and the computations were performed with $L = 100$, $M = 250$, $A = 3M$ and $B = 3L$ in each case. The resulting free-streamline profiles are shown in figures 5(*a*)–5(*c*).

https://doi.org/10.1017/S0022112096004399 Published online by Cambridge University Press

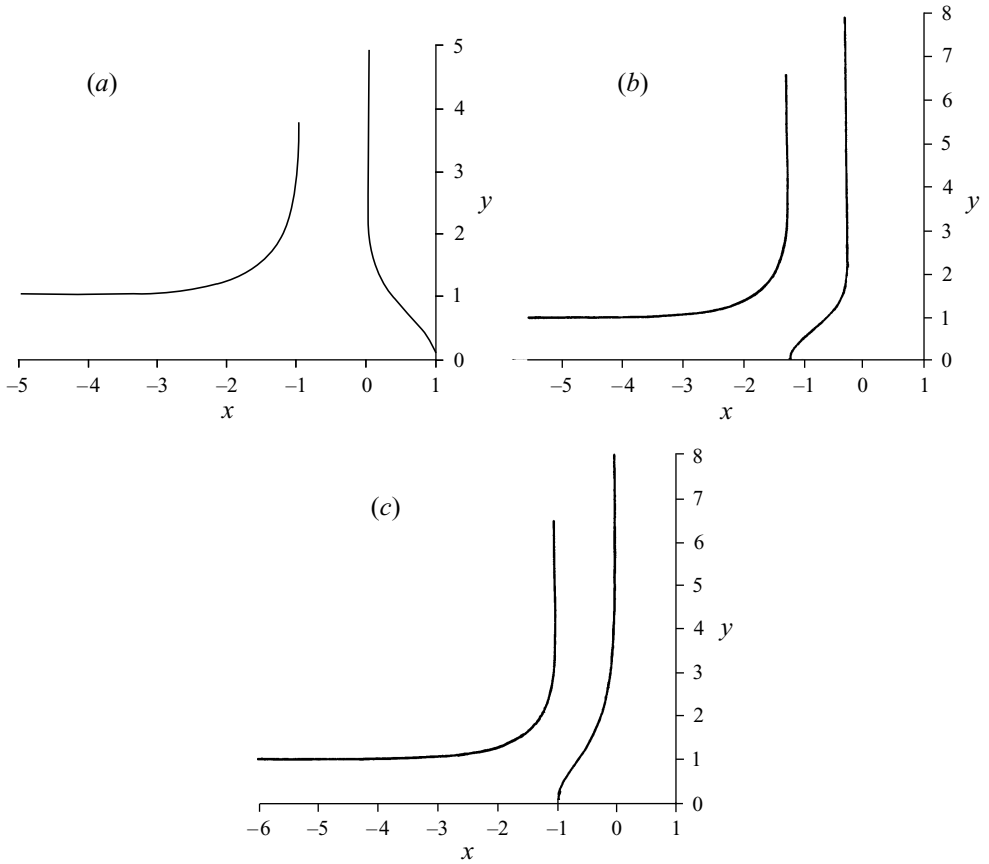


FIGURE 5. A jet of upstream width 2 impinging symmetrically on an uneven wall given by: (*a*) $x = \mathrm{e}^{-y^2}$, (*b*) $x = -\mathrm{e}^{-y^2}$, (*c*) $x = -\mathrm{sech}y$.

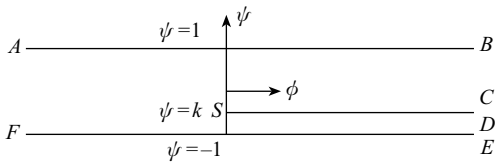


FIGURE 6. The w-plane for a jet impinging on an asymmetric wall.

7. Asymmetric cases

We assume that the flow has only one stagnation point S in the physical plane, the Z-plane (see figure 1). In the plane of the non-dimensional complex potential this corresponds to $w = k\mathrm{i}$ (see figure 6), where $\mathrm{d}w/\mathrm{d}z = 0$.

In the reference ζ-plane (see figure 2), it is labelled as $\zeta = a$ with

$$v \sim (\zeta - a)v_0 \qquad \text{as} \quad \zeta \to a$$

provided that the boundary is smooth at S. (If the wall Γ has a corner of angle β_1 at S, then $v \sim v_0(\zeta - a)^{\beta_1/\pi}$.) In general, the expression for ω in (2.2) has singularity term

$$\frac{\beta_1}{\pi}\log(\zeta - a), \tag{7.1}$$

https://doi.org/10.1017/S0022112096004399 Published online by Cambridge University Press

so that it is readily shown that $\log q \in L_2[-\infty, \infty]$. Therefore we obtain, from the reciprocity theorem (see Tricomi 1957; Hochstadt 1973), the reciprocity formulae

$$\log q(\xi) = \frac{1}{\pi} \int_{-\infty}^{\infty} \frac{\theta(t)}{\xi - t} \mathrm{d}t, \quad \theta(\xi) = -\frac{1}{\pi} \int_{-\infty}^{\infty} \frac{\log q(t)}{\xi - t} \mathrm{d}t. \tag{7.2}$$

By application of the Bernoulli condition, we have $\log q = 0$ on $\eta = 0$, $|\xi| > 1$ so that equation (7.2) can be reduced to

$$\theta(\xi) = -\frac{1}{\pi} \int_{-1}^{1} \frac{\log q}{\xi - t} \mathrm{d}t, \qquad |\xi| < \infty, \tag{7.3}$$

where the integral is a Cauchy principal value integral on $|\xi| < 1$.

The transformation which maps the upper half-ζ-plane to the complex potential plane is given as

$$w(\zeta) = -\frac{1+a}{\pi} \log \frac{1+\zeta}{1+a} - \frac{1-a}{\pi} \log \frac{\zeta - 1}{1-a} + \mathrm{i} \tag{7.4}$$

so that the line SC in figure 6 is given by $\Psi = a = 1 - 2H_1/H = (H_2 - H_1)/(H_1 + H_2)$, showing that $k = a$. However the parameter a is unknown. To determine this parameter, the momentum equation for two-dimensional flow of an incompressible inviscid fluid with gravitational effects neglected is taken in the form

$$\rho \oint_{\tau} (\boldsymbol{u} \cdot \boldsymbol{l}) \boldsymbol{u} \cdot \boldsymbol{n} \, \mathrm{d}s = -\oint_{\tau} p \, \boldsymbol{l} \cdot \boldsymbol{n} \, \mathrm{d}s \tag{7.5}$$

where $\boldsymbol{u}$ is the velocity, p the pressure, ρ the density and τ denotes a closed curve with outward normal $\boldsymbol{n}$, while $\boldsymbol{l}$ is an arbitrary constant vector.

For a jet impinging on an asymmetric uneven wall, τ is taken as the 'control surface' corresponding to the curve τ shown dashed in figure 1, consisting of two free streamlines, the wall Γ and lines at right angles to the flow directions at infinity. Taking OX parallel to the incoming stream, so that the two outgoing streams are inclined at angles α and γ, respectively, to the OY-axis, the choice of $\boldsymbol{l}$ as the unit vector $\boldsymbol{l} = (\sin\beta, \cos\beta)$ then gives

$$\rho U^2(-2H \sin\beta + H_1 \cos(\beta - \alpha) - H_2 \cos(\gamma - \beta)) = -\int_{\dot{\tau}} p \; \boldsymbol{n} \cdot \boldsymbol{l} \, \mathrm{d}s - \int_{\ddot{\tau}} p_0 \; \boldsymbol{n} \cdot \boldsymbol{l} \, \mathrm{d}s \tag{7.6}$$

where $\dot{\tau}$ is the wetted portion of the wall CSD, and $\ddot{\tau}$ includes the surfaces DE, EF, FA, AB and BC in figure 1 on which the pressure has the uniform value p_0. Since $\tau = \dot{\tau} + \ddot{\tau}$ is a closed surface, we obtain

$$\oint_{\tau} p_0 \, \boldsymbol{n} \cdot \boldsymbol{l} \, \mathrm{d}s = 0$$

which converts (7.6) to

$$\sin\beta - \tfrac{1}{2}(1-a)\cos(\beta - \alpha) + \tfrac{1}{2}(1+a)\cos(\gamma - \beta) = \frac{1}{2} \int_{\dot{\tau}} (\rho U^2 H)^{-1} (p - p_0) \boldsymbol{n} \cdot \boldsymbol{l} \, \mathrm{d}s, \tag{7.7}$$

since $H_1/H = 1 - a$, $H_2/H = 1 + a$. Using the Bernoulli equation

$$p - p_0 = \tfrac{1}{2}(1 - q^2(\xi)), \qquad |\xi| < 1,$$

and noting that along the wall given by $x = k(y)$ we have

$$\boldsymbol{n} = (n_1, n_2) = (1 + k'^2)^{-1/2} \left(1, \; -k'\right), \qquad H^{-1} \mathrm{d}s = (1 + k'^2)^{1/2} \mathrm{d}y,$$

https://doi.org/10.1017/S0022112096004399 Published online by Cambridge University Press

we obtain from (7.7) the pair of conditions

$$2-(1-a)\sin\alpha+(1+a)\sin\gamma=\int_{-1}^{1}(1-q^2)y'(\xi)\mathrm{d}\xi, \tag{7.8}$$

$$-(1+a)\cos\gamma+(1-a)\cos\alpha=\int_{-1}^{1}(1-q^2)k'y'(\xi)\mathrm{d}\xi. \tag{7.9}$$

These arise from the choices $\beta=\pi/2$ and $\beta=0$, corresponding to momentum conservation in the OX- and OY-directions, respectively. In the special case $\alpha=\gamma=0$, these yield

$$2=\int_{-1}^{1}(1-q^2)y'(\xi)\mathrm{d}\xi, \tag{7.10}$$

$$2a=-\int_{-1}^{1}(1-q^2)k'y'(\xi)\mathrm{d}\xi. \tag{7.11}$$

The relation between the flow angle and the slope of the tangent is

$$\theta(\xi)=\begin{cases}\frac{1}{2}\pi-\tan^{-1}k'(y), & a<\xi<1\\ -\frac{1}{2}\pi-\tan^{-1}k'(y), & -1<\xi<a\end{cases}. \tag{7.12}$$

The integral equation (7.3) for $|\xi|<1$ can be inverted using the finite Hilbert transform in terms of $\theta(\xi)$. We obtain

$$\log q=-\frac{1}{\pi}\fint_{-1}^{1}\left(\frac{1-t^2}{1-\xi^2}\right)^{1/2}\frac{\theta(t)}{t-\xi}\mathrm{d}t+\frac{c}{(1-\xi^2)^{1/2}},\qquad |\xi|<1,$$

where the constant c is obtained by multiplying by $(1-\xi^2)^{1/2}$ and letting $\xi\to1$, so that

$$c=\frac{1}{\pi}\fint_{-1}^{1}(1-t^2)^{1/2}\frac{\theta(t)}{t-1}\mathrm{d}t.$$

Consequently, substituting for c and rearranging gives

$$\begin{aligned}q&=\exp\left\{-\frac{1}{\pi}\fint_{-1}^{1}\left(\frac{1-t^2}{1-\xi^2}\right)^{1/2}\left(\frac{1}{t-\xi}-\frac{1}{t-1}\right)\theta(t)\mathrm{d}t\right\}\\&=\exp\left\{-\frac{1}{\pi}\left(\frac{1-\xi}{1+\xi}\right)^{1/2}\fint_{-1}^{1}\left(\frac{1+t}{1-t}\right)^{1/2}\frac{\theta(t)}{t-\xi}\mathrm{d}t\right\},\qquad |\xi|<1.\end{aligned} \tag{7.13}$$

The variable y is specified using equation (4.2) as

$$\frac{\mathrm{d}y}{\mathrm{d}\xi}=-\frac{2}{\pi}\frac{\xi-a}{\xi^2-1}(q(\xi))^{-1}\sin\theta(\xi),\qquad |\xi|<\infty,$$

which may be integrated to show that on the wall y is related to θ and q by

$$y(\xi)=-1-\frac{2}{\pi}\int_{-\infty}^{\xi}\frac{t-a}{t^2-1}(q(t))^{-1}\sin\theta(t)\mathrm{d}t,\qquad |\xi|<1. \tag{7.14}$$

The problem now is governed by a system of equations (7.3), (7.7), (7.11), (7.12) and (7.14). When the system of equations is solved, we obtain $q(\xi)$, $|\xi|<1$ and the parameter a. Equation (7.3) gives the flow angles both on the wall and on the free

https://doi.org/10.1017/S0022112096004399 Published online by Cambridge University Press

surface. Therefore we consider (4.5) and obtain

$$\frac{\mathrm{d}z}{\mathrm{d}\xi} = -\frac{2}{\pi}\frac{\xi - a}{\xi^2 - 1}\exp(\mathrm{i}\theta(\xi)), \qquad |\xi| > 1.$$

Taking the real and imaginary parts and integrating then yields

$$x(\xi) = x(\xi_0) - \frac{2}{\pi}\int_{\xi_0}^{\xi} \frac{t-a}{t^2-1}\cos\theta(t)\mathrm{d}t, \qquad |\xi| > 1, \tag{7.15}$$

$$y(\xi) = -1 - \frac{2}{\pi}\int_{-\infty}^{\xi} \frac{t-a}{t^2-1}\sin\theta(t)\mathrm{d}t, \qquad |\xi| > 1 \tag{7.16}$$

where $x(\xi_0)$ is assumed to be given. These equations then give the shape of the free surface.

8. Linearization of the problem

If the wall function is $x = \epsilon k(y)$, $\epsilon \ll 1$, then the wall angle θ_w may be written as

$$\begin{aligned}\theta_w(t) &= \tfrac{1}{2}\pi - \tan^{-1}\epsilon k'(y(t)) \\ &= \tfrac{1}{2}\pi - \epsilon k'(y(t)) + O(\epsilon^2),\end{aligned}$$

so giving the flow angle along the wall as

$$\theta(t) = \begin{cases} \frac{1}{2}\pi - \epsilon k'(y(t)) + O(\epsilon^2), & a < t < 1 \\ -\frac{1}{2}\pi - \epsilon k'(y(t)) + O(\epsilon^2), & -1 < t < a. \end{cases} \tag{8.1}$$

If we write

$$\begin{aligned} y(t) &= y_0(t) + \epsilon y_1(t) + O(\epsilon^2), && |t| < 1, \\ q(t) &= q_0(t) + \epsilon q_1(t) + O(\epsilon^2), && |t| < 1, \\ \theta(t) &= \theta_0(t) + \epsilon\theta_1(t) + O(\epsilon^2), && |t| < \infty, \\ a &= a_0 + \epsilon a_1 + O(\epsilon^2) \end{aligned}$$

then substituting into equation (7.11) gives

$$a_0 = 0, \qquad a_1 = -\int_{-1}^{1}(1 - q_0^2(t))k'(y_0(t))y_0'(t)\mathrm{d}t. \tag{8.2}$$

Thus, since equation (8.1) shows that $\theta_0(t) = \frac{1}{2}\pi$ for $0 < t < 1$ and $\theta_0(t) = -\frac{1}{2}\pi$ for $-1 < t < 0$, equations (7.13) and (7.14) yield

$$q_0(t) = \left|\frac{(1+t)^{1/2} - (1-t)^{1/2}}{(1+t)^{1/2} + (1-t)^{1/2}}\right|, \quad y_0(t) = \tfrac{1}{2}\log\frac{1+t}{1-t} - 2\tan^{-1}\left(\frac{1-t}{1+t}\right)^{1/2} + \tfrac{1}{2}\pi. \tag{8.3}$$

The function $F(\xi)$ of equation (3.2) is given by

$$\begin{aligned} F(\xi) &= \frac{1}{\pi}\left[\int_a^1 \frac{\frac{1}{2}\pi}{\xi - t}\mathrm{d}t - \epsilon\int_a^1 \frac{k'(y(t))}{\xi - t}\mathrm{d}t \right. \\ &\qquad \left. + \int_{-1}^{a}\frac{-\frac{1}{2}\pi}{\xi - t}\mathrm{d}t - \epsilon\int_{-1}^{a}\frac{k'(y(t))}{\xi - t}\mathrm{d}t + O(\epsilon^2)\right] \\ &= \frac{1}{2}\log\frac{(\xi - a)^2}{\xi^2 - 1} - \frac{\epsilon}{\pi}\int_{-1}^{1}\frac{k'(y(t))}{\xi - t}\mathrm{d}t + O(\epsilon^2) \\ &= F_0(\xi) + \epsilon F_1(\xi) + O(\epsilon^2) \end{aligned} \tag{8.4}$$

https://doi.org/10.1017/S0022112096004399 Published online by Cambridge University Press

with

$$F_0(\xi) = \frac{1}{2}\log\frac{\xi^2}{\xi^2-1}, \qquad F_1(\xi) = \frac{1}{\pi}\int_{-1}^{1}\frac{k'(y_0(t))}{\xi - t}\mathrm{d}t - \frac{a_1}{\xi}, \tag{8.5}$$

which yields from equation (3.12) the expression

$$\theta_j(t) = \pm\frac{(t^2-1)^{1/2}}{t}\left(\int_{-\infty}^{-1} - \int_{1}^{\infty}\right)\frac{\xi}{(\xi^2-1)^{1/2}}\frac{F_j(\xi)}{\xi - t}\mathrm{d}\xi, \qquad |\xi| > 1. \tag{8.6}$$

These may be used for any wall profile $x = \epsilon k(y)$. Taking into account results (8.2), this gives

$$x(\xi) = x(\xi_0) - \frac{2}{\pi}\int_{\xi_0}^{\xi}\frac{t}{t^2-1}\cos\theta_0(t)\mathrm{d}t + \frac{2\epsilon}{\pi}\int_{\xi_0}^{\xi}\frac{a_1\cos\theta_0(t) + t\theta_1(t)\theta_0'(t)\sin\theta_0(t)}{t^2-1}\mathrm{d}t, \qquad |\xi| > 1, \tag{8.7}$$

$$y(\xi) = -1 - \frac{2}{\pi}\int_{-\infty}^{\xi}\frac{t}{t^2-1}\sin\theta_0(t)\mathrm{d}t + \frac{2\epsilon}{\pi}\int_{-\infty}^{\xi}\frac{a_1\sin\theta_0(t) - t\theta_1(t)\theta_0'(t)\cos\theta_0(t)}{t^2-1}\mathrm{d}t, \qquad |\xi| > 1 \tag{8.8}$$

as parametric expressions for the free-surface shape. This solution provides us an approximation to the full system and also gives the starting point for computing the shape of the free surface corresponding to the full problem.

9. The inclined plane wall – a special case

For a jet impinging on an inclined flat wall with $x = k(y) = y\tan\alpha$ so that $k'(y) = \tan\alpha$, the choice $\beta = \alpha = \gamma$ in (7.7) shows that $a = -\sin\alpha$. Using these in equations (7.12) and (7.13) then gives

$$q = \exp\left\{\frac{1}{\pi}\left[\int_{-1}^{-\sin\alpha}\left(\frac{1-t^2}{1-\xi^2}\right)^{1/2}\frac{\frac{1}{2}\pi + \alpha}{t-\xi}\mathrm{d}t - \int_{-\sin\alpha}^{1}\left(\frac{1-t^2}{1-\xi^2}\right)^{1/2}\frac{\frac{1}{2}\pi - \alpha}{t-\xi}\mathrm{d}t\right] - \frac{\cos\alpha}{(1-\xi^2)^{1/2}}\right\}, \qquad |\xi| < 1. \tag{9.1}$$

In (9.1), the first integral is found by the substitution $t = \cos t_1$ (where t_1 is a dummy variable) to be

$$I_1 = \frac{\frac{1}{2}\pi + \alpha}{(1-\xi^2)^{1/2}}\int_{-1}^{-\sin\alpha}\frac{(1-t^2)^{1/2}}{t-\xi}\mathrm{d}t = \frac{\frac{1}{2}\pi + \alpha}{(1-\xi^2)^{1/2}}\left(\cos\alpha - \xi\left(\tfrac{1}{2}\pi - \alpha\right) - (1-\xi^2)^{1/2}F(r)\right) \tag{9.2}$$

where

$$r = \left(\frac{1-\xi}{1+\xi}\right)^{1/2}, \qquad F(r) = \log\left|\frac{1 + r\tan(\frac{1}{4}\pi - \frac{1}{2}\alpha)}{1 - r\tan(\frac{1}{4}\pi - \frac{1}{2}\alpha)}\right|. \tag{9.3}$$

https://doi.org/10.1017/S0022112096004399 Published online by Cambridge University Press

Similarly the second integral is obtained as

$$I_2 = \frac{\frac{1}{2}\pi - \alpha}{(1-\xi^2)^{1/2}}\left(-\cos\alpha - \xi\left(\tfrac{1}{2}\pi + \alpha\right) + (1-\xi^2)^{1/2}F(r)\right). \tag{9.4}$$

This may be combined with (9.2) using (9.3) and inserted into (9.1) to give

$$q(\xi) = \exp\left\{\frac{I_1 - I_2}{\pi} - \frac{\cos\alpha}{(1-\xi^2)^{1/2}}\right\} = \exp\{-F(r)\} = \exp\left\{-F\left[\left(\frac{1-\xi}{1+\xi}\right)^{1/2}\right]\right\}.$$

This is best writtten in terms of $\bar{\alpha} = \pi/2 - 2\tan^{-1} r$, since (9.3) then shows that $\xi = \sin\bar{\alpha}$ and

$$q(\xi) = q(\sin\bar{\alpha}) = \left|\frac{1 - \tan(\frac{1}{4}\pi - \frac{1}{2}\bar{\alpha})\tan(\frac{1}{4}\pi - \frac{1}{2}\alpha)}{1 + \tan(\frac{1}{4}\pi - \frac{1}{2}\bar{\alpha})\tan(\frac{1}{4}\pi - \frac{1}{2}\alpha)}\right| = \frac{\left|\sin\frac{1}{2}(\bar{\alpha} + \alpha)\right|}{\cos\frac{1}{2}(\bar{\alpha} - \alpha)}, \tag{9.5}$$

which checks with the statement that the stagnation point occurs where $\xi = \sin(-\alpha) = -\sin\alpha$.

From equations (9.5) and (7.3) the expression for $\theta(\xi)$ may be evaluated and the corresponding shape of the free surface determined by using (7.15) and (7.16). These may be used like expressions (8.3)–(8.5) to give initial approximations for jets impinging on a curved wall from an inclined angle.

10. The numerical scheme

The integration within equation (7.13) is written as

$$\begin{aligned}
&\int_{-1}^{a-\epsilon_1}\left(\frac{1-t^2}{1-\xi^2}\right)^{1/2}\left(\frac{1}{t-\xi} - \frac{1}{t-1}\right)\theta(t)\mathrm{d}t \\
&\quad + \int_{a-\epsilon_1}^{a+\epsilon_2}\left(\frac{1-t^2}{1-\xi^2}\right)^{1/2}\left(\frac{1}{t-\xi} - \frac{1}{t-1}\right)\theta(t)\mathrm{d}t \\
&\quad + \int_{a+\epsilon_2}^{1}\left(\frac{1-t^2}{1-\xi^2}\right)^{1/2}\left(\frac{1}{t-\xi} - \frac{1}{t-1}\right)\theta(t)\mathrm{d}t \equiv J_1 + J_2 + J_3, \quad |\xi| < 1.
\end{aligned} \tag{10.1}$$

At $\xi = a$, the flow angle θ has a jump, so that

$$\theta(t) \simeq \begin{cases} \beta_0, & a < \xi < a + \epsilon_2 \\ \beta_0 - \pi, & a - \epsilon_1 < \xi < a\,. \end{cases} \tag{10.2}$$

In J_2, the first term can be approximated using (10.2) as

$$\begin{aligned}
&\int_{a-\epsilon_1}^{a+\epsilon_2}\left(\frac{1-t^2}{1-\xi^2}\right)^{1/2}\frac{\theta(t)}{t-\xi}\mathrm{d}t \\
&\simeq \frac{1}{(1-\xi^2)^{1/2}}\left[(\beta_0 - \pi)\int_{a-\epsilon_1}^{a}\frac{(1-t^2)^{1/2}}{t-\xi}\mathrm{d}t + \beta_0\int_{a}^{a+\epsilon_2}\frac{(1-t^2)^{1/2}}{t-\xi}\mathrm{d}t\right] \\
&= \frac{1}{(1-\xi^2)^{1/2}}\left[\beta_0(\sin u_2 - \sin u_1) + \pi(\sin u_1 - \sin u_0) + \xi(\beta_0(u_2 - u_1) + \pi(u_1 - u_0))\right] \\
&\quad - \left(\beta_0\log\left|\frac{r + \tan\frac{1}{2}u_2}{r - \tan\frac{1}{2}u_2}\right| - \beta_0\log\left|\frac{r + \tan\frac{1}{2}u_1}{r - \tan\frac{1}{2}u_1}\right|\right. \\
&\qquad \left. + \pi\log\left|\frac{r + \tan\frac{1}{2}u_1}{r - \tan\frac{1}{2}u_1}\right| - \pi\log\left|\frac{r + \tan\frac{1}{2}u_0}{r - \tan\frac{1}{2}u_0}\right|\right)
\end{aligned} \tag{10.3}$$

https://doi.org/10.1017/S0022112096004399 Published online by Cambridge University Press

where

$$\cos u_0 = a, \quad \cos u_1 = a - \epsilon_1, \qquad \cos u_2 = a + \epsilon_2. \tag{10.4}$$

Equation (10.3) shows that as $\xi \to a$,

$$r = \left(\frac{1-\xi}{1+\xi}\right)^{1/2} \to \left(\frac{1-a}{1+a}\right)^{1/2} = \tan \tfrac{1}{2}u_0,$$

giving $J_2 \to -\infty$. Therefore $q(\xi) \to 0$, which is consistent with $q(a) = 0$.

The singularities of (10.1) at $\xi = \pm 1$ can be treated in a similar way. The variables in the two integrals are changed, for convenience of computation, using two different transformations. In J_1, let

$$(1+a)u_1 = 1 + t, \quad \mathrm{d}t = (1+a)\mathrm{d}u_1$$

and in J_3, let

$$(1-a)u_2 = t - a, \quad \mathrm{d}t = (1-a)\mathrm{d}u_2.$$

Then as $\epsilon_1 \to 0$ and $\epsilon_2 \to 0$, the other two integrals in equation (10.1) are changed to

$$\begin{aligned}\lim(J_1 + J_3) = {} & \left(\frac{1-\xi}{1+\xi}\right)^{1/2} \int_0^1 \left(\frac{(1+a)u_1}{2-(1+a)u_1}\right)^{1/2} \frac{\theta((1+a)u_1 - 1))}{(1+a)u_1 - 1 - \xi}(1+a)\mathrm{d}u_1 \\ & + \left(\frac{1-\xi}{1+\xi}\right)^{1/2} \int_0^1 \left(\frac{1+a+(1-a)u_2}{(1-a)(1-u_2)}\right)^{1/2} \frac{\theta((1-a)u_2 + a))}{(1-a)u_2 + a - \xi}(1-a)\mathrm{d}u_2, \\ & |\xi| < 1. \end{aligned} \tag{10.5}$$

Since u_1 and u_2 are dummy variables, using u to replace them in (10.5) gives

$$\begin{aligned}\lim(J_1 + J_3) = {} & \left(\frac{1-\xi}{1+\xi}\right)^{1/2} \int_0^1 \left(\frac{(1+a)u}{2-(1+a)u}\right)^{1/2} \frac{\theta_1(u)(1+a)}{(1+a)u - 1 - \xi}\mathrm{d}u \\ & + \left(\frac{1-\xi}{1+\xi}\right)^{1/2} \int_0^1 \left(\frac{1+a+(1-a)u}{(1-a)(1-u)}\right)^{1/2} \frac{\theta_2(u)(1-a)}{(1-a)u + a - \xi}\mathrm{d}u, \\ & |\xi| < 1 \end{aligned} \tag{10.6}$$

where

$$\theta_1(u) = \theta((1+a)u - 1), \qquad \theta_2(u) = \theta((1-a)u + a) \quad .$$

Using a collocation method to treat the integrations over $(-1, 1)$ numerically, the interval $[-1, 1]$ is divided into $[-1, a)$ and $(a, 1]$ for which two different discretizations are introduced as

$$\left.\begin{array}{ll} t_i = (1+a)ih_1 - 1, & i = 0, \cdots, M, \quad Mh_1 = 1 \quad \text{on} \quad [-1, a), \\ t_i = a + (i-M)h_2(1-a), & i = M+1, \cdots, N, \quad (N-M)h_2 = 1 \quad \text{on} \quad (a, 1]. \end{array}\right\} \tag{10.7}$$

This scheme applied to (10.6) then gives an approximation to (7.13) which expresses the flow speed along the wall as a function of flow angle θ in a discrete form. In the following method, all the integrals over $(-1, 1)$ will be treated using this scheme.

To seek the discrete form of (7.14) which is expressed in term of q and $\theta(\xi)$, we

https://doi.org/10.1017/S0022112096004399 Published online by Cambridge University Press

first consider the discrete form of equation (7.3) for $|\xi| > 1$:

$$\theta(\xi) = \frac{1}{\pi}\int_{-1}^{1}\frac{\log q}{\xi - t}\mathrm{d}t$$
$$\simeq \frac{1}{\pi}\left[h_1(1+a)\sum_{i=1}^{M}\frac{\log q(t_i)}{\xi - t_i} + h_2(1-a)\sum_{i=M+1}^{N}\frac{\log q(t_i)}{\xi - t_i}\right]. \tag{10.8}$$

The integral in equation (7.14) is divided into three parts:

$$y(\xi) = -1 - \frac{2}{\pi}\left[\int_{-\infty}^{-1-\epsilon}\frac{t-a}{t^2-1}\sin\theta(t)\mathrm{d}t + \int_{-1-\epsilon}^{-1+\epsilon}\frac{t-a}{t^2-1}(q(t))^{-1}\sin\theta(t)\mathrm{d}t\right.$$
$$\left.\int_{-1+\epsilon}^{\xi}\frac{t-a}{t^2-1}(q(t))^{-1}\sin\theta(t)\mathrm{d}t\right], \quad |\xi| < 1 \tag{10.9}$$

where $q = 1$ has been used in the first integrand.

Since, as $\xi \to -1$,

$$q \to 1, \qquad \theta \to \gamma,$$

the second integration is approximated by

$$\int_{-1-\epsilon}^{-1+\epsilon}\frac{t-a}{t^2-1}\sin\gamma\ \ \mathrm{d}t = \frac{1-a}{2}\sin\gamma\log\frac{2-\epsilon}{2+\epsilon}.$$

The other two integrals are evaluated in different ways. The first integral is further divided into

$$\int_{-\infty}^{-1-\epsilon}\frac{t-a}{t^2-1}\sin\theta(t)\mathrm{d}t = \int_{-\infty}^{-1-\epsilon}\frac{t}{t^2-1}\sin\theta(t)\mathrm{d}t - a\int_{-\infty}^{-1-\epsilon}\frac{1}{t^2-1}\sin\theta(t)\mathrm{d}t.$$

Using the transformations

$$\log(t^2-1) = \xi_1, \qquad \log\frac{t-1}{t+1} = \xi_2$$

in the integrals respectively gives

$$\int_{-\infty}^{-1-\epsilon}\frac{t-a}{t^2-1}\sin\theta(t)\mathrm{d}t = \frac{1}{2}\int_{\log\epsilon(2+\epsilon)}^{\infty}\sin\theta\left(-(1+\mathrm{e}^{\xi_1})^{1/2}\right)\mathrm{d}\xi_1$$
$$-\frac{a}{2}\int_{0}^{\log(2+\epsilon)/\epsilon}\sin\theta\left(\frac{1+\mathrm{e}^{\xi_2}}{1-\mathrm{e}^{\xi_2}}\right)\mathrm{d}\xi_2$$

where θ is evaluated using (10.8). For the third integral in (10.9), the scheme (10.7) is employed. In the case $\xi < a$, we obtain $\xi = \xi_j$, $j = 1, \cdots, M$

$$\int_{-1+\epsilon}^{\xi}\frac{t-a}{t^2-1}(q(t))^{-1}\sin\theta(t)\mathrm{d}t = h_1(1+a)\sum_{i=1}^{j}\frac{\xi_i - a}{\xi_i^2 - 1}(q(\xi_i))^{-1}\sin\theta(\xi_i).$$

In the case that $\xi > a$, $\xi = \xi_j$, $j = M+1, \cdots, N$, the integral is also split into two

https://doi.org/10.1017/S0022112096004399 Published online by Cambridge University Press

parts as

$$\int_{-1+\epsilon}^{\xi} \frac{t-a}{t^2-1}(q(t))^{-1}\sin\theta(t)\mathrm{d}t = h_1(1+a)\sum_{i=1}^{M}\frac{\xi_i-a}{\xi_i^2-1}(q(\xi_i))^{-1}\sin\theta(\xi_i) + h_2(1-a)\sum_{M+1}^{j}\frac{\xi_i-a}{\xi_i^2-1}(q(\xi_i))^{-1}\sin\theta(\xi_i).$$

Equation (7.7) is discretized as

$$\left(-(\sin\beta+\cos(\gamma-\beta))+\frac{1-a}{2}(\cos(\beta-\alpha)+\cos(\gamma-\beta))\right) = \frac{1}{2}\left[h_1(1+a)\sum_{i=0}^{M}(1-q_i^2)(\sin\beta-K'(y_i)\cos\beta)P_i + h_2(1-a)\sum_{i=M+1}^{N}(1-q_i^2)(\sin\beta-K'(y_i)\cos\beta)P_i\right], \tag{10.10}$$

where

$$y_i = y(\xi_i), \qquad P_i = \frac{\xi_i-a}{\xi_i^2-1}(q(\xi_i))^{-1}\sin\theta(\xi_i). \tag{10.11}$$

The discretized forms of (7.8) and (7.9) are obtained by simply letting $\beta = \frac{1}{2}\pi$ and $\beta = 0$. Since we have

$$y(\xi_j) = -1 - \frac{2}{\pi}\int_{-\infty}^{\xi_j}\frac{\sin\theta(t)}{q(t)}\mathrm{d}t, \qquad |\xi_j| < 1 \tag{10.12}$$

for $j = 1, 2, \cdots, N-1$, then substituting these into (7.12) yields

$$\theta(\xi_j) = \begin{cases} -\frac{1}{2}\pi - \tan^{-1}k'(y(\xi_j)), & j = 1, \cdots, M \\ \frac{1}{2}\pi - \tan^{-1}k'(y(\xi_j)), & j = M+1, \cdots, N-1. \end{cases} \tag{10.13}$$

These equations and (10.10) constitute N algebraic equations containing N unknowns $\theta(\xi_1), \cdots, \theta(\xi_{N-1})$ and the parameter a. The profile of the free surface is obtained from equations (7.15) and (7.16).

11. Results

The method is tested by considering a few different types of wall shape. For instance, $x(y) = -c\mathrm{e}^{-(y-b)^2}$ and $x(y) = -(c/2)\mathrm{sech}(y-b)$ where c and b can be chosen. In the case $b = 0$, the wall shapes become symmetrical about the x-axis and, we found that when $|c| < 1$, the results agree very well with the results obtained by using the method developed for the symmetric wall shapes. We found that as b increases slightly, the jet flowing to $y \to -\infty$ is wider than the jet flowing to $y \to \infty$. In figure 7, the linearized solution given in §8 is compared to the numerical solution of the system of equations. This plot shows that for $\epsilon = 0.25$, the linear approximation agrees quite well with the nonlinear solution. However, in figure 8, we show the difference between a solution of the linearized problem and the nonlinear solution as the steepness parameter c increases, where the shape of the wall is given by $x(y) = -0.5\mathrm{e}^{-(y-0.5)^2}$. Figure 9(*a*) shows us that as the centreline of the incoming jet moves away from the

https://doi.org/10.1017/S0022112096004399 Published online by Cambridge University Press

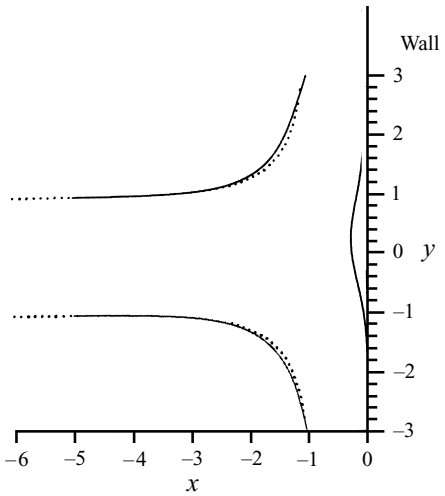


FIGURE 7. The shape of the free surface of a jet flow impinging on wall $x(y) = -0.25e^{-(y-0.2)^2}$. The dotted lines represent the linearized solution. The solid lines represent the numerical solution of the full system.

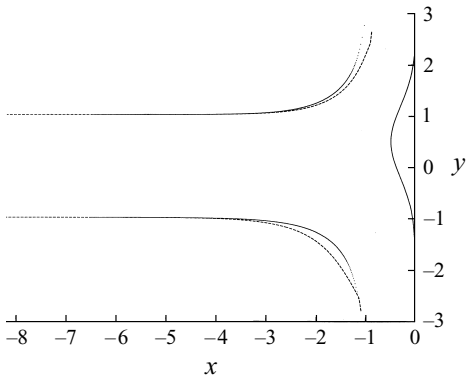


FIGURE 8. The shape of the free surface of a jet flow impinging on wall $x(y) = -0.5e^{-(y-0.5)^2}$. The dotted lines represent the linearized solution. The broken lines represent the numerical solution of the full system.

midpoint of the wall, the upward flow of fluid is blocked. The discrepancy between the widths of the two outgoing jets is given by $2|a|$, where a is determined as part of the solution. Figure 9(b) provides more evidence that the different widths of the two outgoing jets depends on the wall shape. As the shape of the wall steepens in figure 9(c), more fluid goes down than up. Further, as c increases from 0.8 in figure 9(c) to 1.2 in figures 9(d) and 9(e), parameter a is fairly sensitive to the offset b. These results show differences from the symmetrical cases where, although the wall becomes steep, the free-surface shape of the impinging jet does not change much.

12. Conclusions

In this study, we have investigated the free-streamline problem for a jet impinging on various walls. A relation between the flow angle on the free surface and the flow angle on the wall is given. In some special cases, this may be reduced to a simple integral

https://doi.org/10.1017/S0022112096004399 Published online by Cambridge University Press

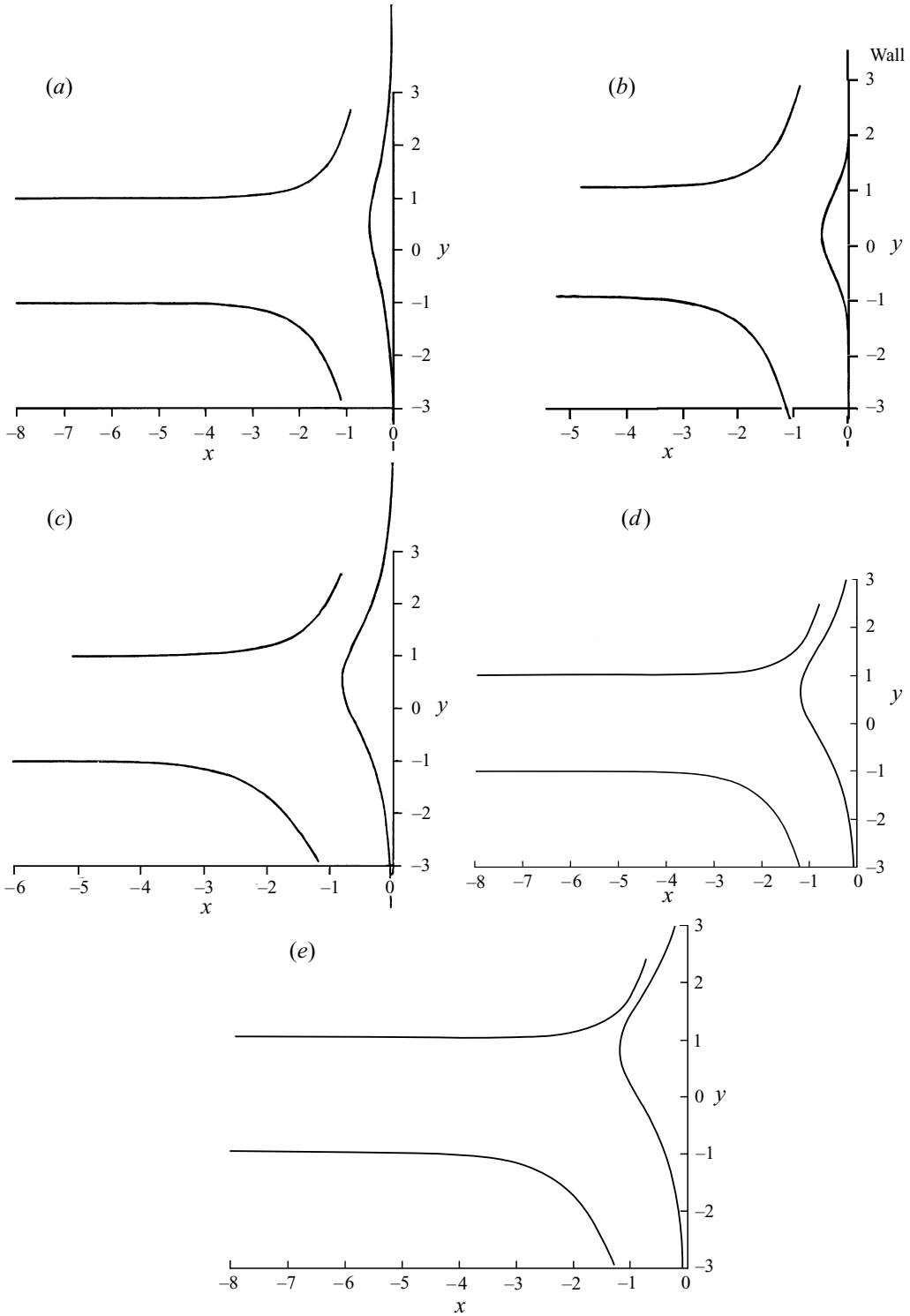


FIGURE 9. Normal incidence upon the wall: (*a*) $x(y) = -0.5\mathrm{sech}(y - 0.5)$, giving $a = 0.0986$; (*b*) $x(y) = -0.5\mathrm{e}^{-(y-0.2)^2}$, giving $a = 0.0797$; (*c*) $x(y) = -0.8\mathrm{sech}(y - 0.5)$, giving $a = 0.1724$; (*d*) $x(y) = -1.2\mathrm{sech}(y - 0.65)$, giving $a = 0.2060$; (*e*) $x(y) = -1.2\mathrm{sech}(y - 0.85)$, giving $a = 0.2460$.

https://doi.org/10.1017/S0022112096004399 Published online by Cambridge University Press

expression. Based on the relation (3.12), a system of equations is formulated which allows for very general boundary shapes. In the special case of a jet impinging normally on a plane wall, the analytic solution, a standard analytic formula (Milne-Thomson 1968) was rederived. The utility of our formulation is tested by comparing the numerical computation for this case with this standard analytic formula, showing good numerical agreement. Calculations for symmetric jets hitting specific curved walls are shown. In the case of unsymmetrical wall shapes, a linearized theory is developed. Numerical solutions are presented, showing the shape of the free surface corresponding to a number of different wall shapes. Further work will deal with jet flow over an uneven wall with surface tension acting on the free surface and for boundary conditions corresponding to porous walls. The formulation allows more freedom than that used by King (1990), since it does not use special properties of the hodograph plane.

We would like to acknowledge the useful comments of the referees. W. P. was supported in this work by an Edinburgh University Postgraduate Studentship and an Overseas Research Student award.

Appendix A

The flow angle $\theta(t)$ on the wall satisfies $|\theta(t)| < \pi$ so that from (3.6) one obtains

$$g(x) \leqslant \frac{1}{\pi}\int_{-1}^{1}\frac{\pi}{1-xt}\mathrm{d}t = G(x) = -\frac{1}{x}\log\frac{1-x}{1+x}. \tag{A 1}$$

To show that $g(x)$ is square integrable, we let $G_1(x) = x^{-1}\log(1-x)$, and then show that $G_1(x)$ is square integrable on $[-1,1]$. $G_1(x)$ has singularities at $x = 0, 1$, but

$$\begin{aligned}\int_{-1}^{1}|G_1(x)|^2\mathrm{d}x &= \int_{-1}^{1}\frac{1}{x^2}(\log(1-x))^2\mathrm{d}x \\ &= \int_{c}^{1}\frac{1}{x^2}(\log(1-x))^2\mathrm{d}x + \int_{-1}^{c}\frac{1}{x^2}(\log(1-x))^2\mathrm{d}x,\end{aligned} \tag{A 2}$$

where c is an arbitrary constant in $(0,1)$. The integrand in the second integral of (A2) is bounded while the first integral may be rearranged as

$$\begin{aligned}I_1 &= \int_{c}^{1}\frac{1}{x^2}(\log(1-x))^2\mathrm{d}x \\ &= \frac{1-c}{c^2}[(\log(1-c))^2] - 2\int_{c}^{1}\frac{(1-x)(\log(1-x))^2}{x^3}\mathrm{d}x - 2\int_{c}^{1}\frac{\log(1-x)}{x^2}\mathrm{d}x\end{aligned} \tag{A 3}$$

where the last integral in (A 3) is

$$\begin{aligned}\int_{c}^{1}\frac{1}{x^2}\ln(1-x)\mathrm{d}x &= \left[\left(-\frac{1}{x}+1\right)\right]_{c}^{1} - \int_{c}^{1}\left(\frac{x-1}{x}\right)\frac{-1}{1-x}\mathrm{d}x \\ &= 0 - \frac{c-1}{c}\ln(1-c) - \int_{c}^{1}\frac{\mathrm{d}x}{x} \\ &= -\frac{c-1}{c}\ln(1-c) + \ln c \\ &= \frac{1}{c}\ln(1-c) + \ln\left(\frac{c}{1-c}\right).\end{aligned} \tag{A 4}$$

https://doi.org/10.1017/S0022112096004399 Published online by Cambridge University Press

The integrands in (A3) are bounded functions on $[c, 1]$. Consequently the integral I_1 is bounded so showing that $G_1(x)$ is square integrable. Similarly, $G_1(-x)$ is square integrable so that $G(x) = -[G_1(x) + G_1(-x)]$ is square integrable.

Appendix B

Since equations (3.8) and (3.9) are equivalent, we treat only equation (3.9). Substituting (3.4) into (3.9) and interpreting ϕ in terms of θ through $\theta(s^{-1}) = s\phi(s)$ gives

$$\xi\theta(\xi) = -\frac{1}{\pi}\left[\fint_{\infty}^{1} \left(\frac{\xi^2-1}{(t^2-1)\xi^2}\right)^{1/2} \frac{\xi g(t^{-1})}{t-\xi}(-\mathrm{d}t) + \fint_{-1}^{-\infty} \left(\frac{\xi^2-1}{(t^2-1)\xi^2}\right)^{1/2} \frac{\xi g(t^{-1})}{t-\xi}\mathrm{d}t\right]. \tag{B 1}$$

For $\xi > 1$, equation (B1) becomes

$$\begin{aligned}\xi\theta(\xi) &= -\frac{1}{\pi}\left[\fint_{1}^{\infty} \left(\frac{\xi^2-1}{(t^2-1)}\right)^{1/2} \frac{g(t^{-1})}{t-\xi}\mathrm{d}t - \fint_{-\infty}^{-1} \left(\frac{\xi^2-1}{(t^2-1)}\right)^{1/2} \frac{g(t^{-1})}{t-\xi}\mathrm{d}t\right] \\ &= \frac{1}{\pi}(\xi^2-1)^{1/2}\left(\fint_{-\infty}^{-1} - \fint_{1}^{\infty}\right) \frac{1}{(t^2-1)^{1/2}} \frac{tF(t)}{t-\xi}\mathrm{d}t, \quad \xi > 1,\end{aligned} \tag{B 2}$$

where $g(t^{-1})$ has been replaced by $tF(t)$. For $\xi < -1$, similarly one obtains

$$\xi\theta(\xi) = -\frac{1}{\pi}(\xi^2-1)^{1/2}\left(\fint_{-\infty}^{-1} - \fint_{1}^{\infty}\right) \frac{1}{(t^2-1)^{1/2}} \frac{tF(t)}{t-\xi}\mathrm{d}t, \quad \xi < -1. \tag{B 3}$$

In the symmetric case, equation (B2) can be written as

$$\begin{aligned}\theta(\xi) &= \frac{(\xi^2-1)^{1/2}}{\pi\xi}\fint_{1}^{\infty} \frac{1}{(t^2-1)^{1/2}}\left(\frac{1}{\xi-t} + \frac{1}{\xi+t}\right) tF(t)\mathrm{d}t \\ &= \frac{(\xi^2-1)^{1/2}}{\pi}\fint_{1}^{\infty} \frac{1}{(t^2-1)^{1/2}} \frac{2t}{\xi^2-t^2}F(t)\mathrm{d}t \\ &= \frac{1}{\pi}\left(\frac{\xi+1}{\xi-1}\right)^{1/2}\fint_{1}^{\infty} \frac{1}{(t^2-1)^{1/2}}\left(\frac{t-1}{\xi-t} + \frac{t+1}{\xi+t}\right) F(t)\mathrm{d}t \\ &= \frac{1}{\pi}\left(\frac{\xi+1}{\xi-1}\right)^{1/2}\fint_{1}^{\infty} \left[\left(\frac{t-1}{t+1}\right)^{1/2} \frac{F(t)}{\xi-t} + \left(\frac{t+1}{t-1}\right)^{1/2} \frac{F(t)}{\xi+t}\right]\mathrm{d}t, \\ &\qquad\qquad 1 < \xi < \infty.\end{aligned} \tag{B 4}$$

Appendix C

We consider

$$\frac{1}{\pi}\oint_{C} \frac{\frac{1}{2}\log\left(1+\mathrm{e}^{-2z}\right)}{\sinh(u-z)}\mathrm{d}z, \qquad -\infty < u < \infty, \tag{C 1}$$

https://doi.org/10.1017/S0022112096004399 Published online by Cambridge University Press

where the path of integration C is chosen as shown in figure 3:

$$C = \begin{cases} C_1, & -R < z < u - \epsilon \\ C_2, & z = u + \epsilon e^{i\alpha}, 0 < \alpha < \pi \\ C_3, & u + \epsilon < z < R \\ C_4, & z = R + i\alpha, 0 < \alpha < \frac{1}{2}\pi \\ C_5, & z = x + i\frac{1}{2}\pi, \epsilon < x < R \\ C_6, & z = i\frac{1}{2}\pi + e^{i\alpha}, 0 > \alpha > -\pi \\ C_7, & z = x + i\frac{1}{2}\pi^-, -R < x < -\epsilon \\ C_8, & z = -R + i\alpha, 0 < \alpha < \frac{1}{2}\pi. \end{cases} \tag{C 2}$$

The integration can be split into eight parts

$$\frac{1}{\pi}\oint_C \frac{\frac{1}{2}\log\left(1+e^{-2z}\right)}{\sinh(u-z)}dz = \frac{1}{2\pi}\left\{\int_{C_1}+\int_{C_2}+\int_{C_3}+\int_{C_4}+\int_{C_5}+\int_{C_6}+\int_{C_7}+\int_{C_8}\frac{\log\left(1+e^{-2z}\right)}{\sinh(u-z)}\right\}dz \tag{C 3}$$

which are calculated individually as

$$I_1 = \int_{C_1}\frac{\log\left(1+e^{-2z}\right)}{\sinh(u-z)}dz = \int_{-R}^{u-\epsilon}\frac{\log\left(1+e^{-2x}\right)}{\sinh(u-x)}dx \tag{C 4}$$

$$I_2 = \int_{C_2}\frac{\log\left(1+e^{-2z}\right)}{\sinh(u-z)}dz = \int_{\pi}^{0}\frac{\log\left(1+e^{-2(u+\epsilon e^{i\alpha})}\right)}{\sinh\left(-\epsilon e^{i\alpha}\right)}i\epsilon e^{i\alpha}d\alpha$$
$$\to i\pi\log(1+e^{-2u}) \quad \text{as } \epsilon \to 0, \tag{C 5}$$

$$I_3 = \int_{u+\epsilon}^{R}\frac{\log\left(1+e^{-2x}\right)}{\sinh(u-x)}dx, \tag{C 6}$$

$$I_4 = \int_{R}^{R+i\frac{1}{2}\pi}\frac{\log\left(1+e^{-2z}\right)}{\sinh(u-z)}dz \to 0 \quad \text{as } R \to \infty, \tag{C 7}$$

$$I_5 = \int_{R}^{\epsilon}\frac{\log\left(1+e^{-2(x+i\frac{1}{2}\pi)}\right)}{\sinh\left(u-(x+i\frac{1}{2}\pi)\right)}dx$$
$$= \int_{R}^{\epsilon}\frac{\log\left(1-e^{-2x}\right)}{-i\cosh(u-x)}dx = -i\int_{\epsilon}^{R}\frac{\frac{1}{2}\log\left(1-e^{-2x}\right)}{\cosh(u-x)}dx, \tag{C 8}$$

$$I_6 = \int_{C_6}\frac{\log\left(1+e^{-2z}\right)}{\sinh(u-z)}dz = \int_{-\pi}^{0}\frac{\log\left(1+e^{-2(i\frac{1}{2}\pi+\epsilon e^{i\alpha})}\right)}{\sinh\left(u-i\frac{1}{2}\pi-\epsilon e^{i\alpha}\right)}i\epsilon e^{i\alpha}d\alpha$$
$$= O(\epsilon\log\epsilon) \to 0 \quad \text{as } \epsilon \to 0, \tag{C 9}$$

$$I_7 = \int_{-\epsilon}^{-R}\frac{\log\left(e^{-2x}-1\right)-i\pi}{-i\cosh(u-x)}dx$$
$$= i\int_{-\epsilon}^{-R}\frac{\log\left(e^{-2x}-1\right)}{\cosh(u-x)}dx + \int_{-\epsilon}^{-R}\frac{\pi}{\cosh(u-x)}dx, \tag{C 10}$$

$$I_8 = \int_{-R+\pi/2}^{-R}\frac{\log\left(1+e^{-2z}\right)}{\sinh(u-z)}dz \to 0 \quad \text{as } R \to \infty. \tag{C 11}$$

https://doi.org/10.1017/S0022112096004399 Published online by Cambridge University Press

Since the integrand in (C1) is analytic within C, the integral is zero, i.e.

$$I = \frac{1}{\pi}\oint_C \frac{\frac{1}{2}\log\left(1+\mathrm{e}^{-2z}\right)}{\sinh(u-z)}\mathrm{d}z = 0 \tag{C 12}$$

giving

$$\begin{aligned} I = &\int_{-R}^{u-\epsilon} \frac{\log\left(1+\mathrm{e}^{-2x}\right)}{\sinh(u-x)}\mathrm{d}x + \int_{\pi}^{0} \frac{\log\left(1+\mathrm{e}^{-2(u+\epsilon\mathrm{e}^{\mathrm{i}\alpha})}\right)}{\sinh\left(-\epsilon\mathrm{e}^{\mathrm{i}\alpha}\right)}\mathrm{i}\epsilon\mathrm{e}^{\mathrm{i}\alpha}\mathrm{d}\alpha \\ &+ \int_{u+\epsilon}^{R} \frac{\log\left(1+\mathrm{e}^{-2x}\right)}{\sinh(u-x)}\mathrm{d}x + \int_{R}^{R+\mathrm{i}\pi/2} \frac{\log\left(1+\mathrm{e}^{-2z}\right)}{\sinh(u-z)}\mathrm{d}z \\ &+ O(\epsilon\log\epsilon) - \mathrm{i}\int_{\epsilon}^{R} \frac{\frac{1}{2}\log\left(1-\mathrm{e}^{-2x}\right)}{\cosh(u-x)}\mathrm{d}x + \mathrm{i}\int_{-\epsilon}^{-R} \frac{\log\left(\mathrm{e}^{-2x}-1\right)}{\cosh(u-x)}\mathrm{d}x \\ &+ \int_{-\epsilon}^{-R} \frac{\pi}{\cosh(u-x)}\mathrm{d}x + \int_{-R+\pi/2}^{-R} \frac{\log\left(1+\mathrm{e}^{-2z}\right)}{\sinh(u-z)}\mathrm{d}z = 0. \end{aligned} \tag{C 13}$$

Letting $\epsilon \to 0$ and $R \to \infty$ and taking real parts of (C 4) yields

$$\int_{-\infty}^{\infty} \frac{\log\left(1+\mathrm{e}^{-2x}\right)}{\sinh(u-x)}\mathrm{d}x + \int_{0}^{-\infty} \frac{\pi}{\cosh(u-x)}\mathrm{d}x = 0. \tag{C 14}$$

REFERENCES

Birkhoff, G. & Zarantonello, E. H. 1957 *Jets, Wakes and Cavities*. Academic.

Bloor, M. I. G. 1978 Large amplitude surface waves. *J. Fluid Mech.* **84**, 167–179.

Dias, F. & Christodoulides, P. 1991 Ideal jet flow under gravity. *Phys. Fluids* A **3**, 1711–1717.

Dias, F., Elcrat, A. R. & Trefethen, L. N. 1987 Ideal jet flow in two dimensions. *J. Fluid Mech.* **185**, 275–288.

Dias, F. & Tuck, E. O. 1991 Weir flows and waterfalls. *J. Fluid Mech.* **230**, 525–539.

Dias, F. & Vanden-Broeck, J.-M. 1990 Flows emerging from a nozzle and falling under gravity. *J. Fluid Mech.* **213**, 465–477.

Dobrovol'skaya, Z. N. 1969 On some problems of similarity flow of fluid with a free surface. *J. Fluid Mech.* **36**, 805–829.

Gurevich, M. I. 1965 *Theory of Jets in an Ideal Fluid*. Academic.

Hochstadt, H. 1973 *Integral Equations*. Wiley-Interscience.

Jenkins, D. R. & Barton, N. G. 1989 Computation of the free surface shape of an inviscid jet incident on a porous wall. *IMA J. Appl. Maths* **41**, 193–206.

King, A. C. 1990 A note on the impact of a jet on a porous wall. *IMA J. Appl. Maths* **45**, 139–146.

King, A. C. & Bloor, M. I. G. 1987 Free surface flow over a step. *J. Fluid Mech.* **182**, 193–208.

King, A. C. & Bloor, M. I. G. 1990 Free streamline flow over curved topography. *Q. Appl. Maths* **48**, 281–293.

Martin, H. 1977 Heat and mass transfer between impinging gas jets and solid surfaces. In *Advances in Heat Transfer* (ed. J. P. Hartneff & T. F. Irvine), Vol. 13, pp. 1–60. Academic.

Milne-Thomson, L. M. 1968 *Theoretical Hydrodynamics* (5th edn). Macmillan & Co Ltd.

Stevens, J. & Webb, B. W. 1992 Measurements of the free surface flow structure under an impinging, free liquid jet. *Trans. ASME J. Heat Transfer* **114**, 79–84.

Tricomi, F. G. 1957 *Integral Equations*. Interscience.

Tuck, E. O. 1987 Efflux from a slit in a vertical wall. *J. Fluid Mech.* **176**, 253-264.

Woods, L. C. 1958 Some generalizations of the Schwartz-Christoffel mapping formula. *Appl. Sci. Res.* **B 7**, 89–101.

Woods, L. C. 1961 *The Theory of Subsonic Plane Flow*. Cambridge University Press.

https://doi.org/10.1017/S0022112096004399 Published online by Cambridge University Press